Fabrication of tapered graded-refractive-index micropillars using ion-implanted-photoresist as an etch mask

Ming Ma[a] and E. Fred Schubert
Department of Electrical, Computer, and Systems Engineering, Rensselaer Polytechnic Institute, Troy, New York 12180

Jaehee Cho[b]
School of Semiconductor and Chemical Engineering, Semiconductor Physics Research Center, Chonbuk National University, Jeonju 561-756, South Korea

Morgan Evans
Varian Semiconductor Business Unit, Applied Materials, Gloucester, Massachusetts 01930

Gi Bum Kim and Cheolsoo Sone
LED Business, Samsung Electronics, Yongin 446-920, South Korea

(Received 17 September 2013; accepted 7 January 2014; published 21 January 2014)

Thermally reflowed photoresist is used as an etch mask in inductively coupled plasma reactive ion etching of dielectric graded-refractive-index (GRIN) coatings. The coatings have varying compositions of TiO_2 and SiO_2 and are used to fabricate GRIN micropillars with tapered sidewalls. The effects of ion implantation on the dry-etch-resistance of photoresist are investigated for Si, N, and Ar ion implantation. Compared with the unimplanted photoresist, the implanted photoresists show enhanced dry-etch-resistance under fluorine chemistry (CHF_3 and O_2). The etch rate of the Si-implanted photoresist is 72% lower than that of the unimplanted photoresist. The measured depth of modification of the photoresist is in good agreement with the trend predicted by ion-implantation-simulation software. Using Si-implanted photoresist as an etch mask, five-layer GRIN micropillars with tapered sidewalls are fabricated. © *2014 American Vacuum Society*. [http://dx.doi.org/10.1116/1.4862547]

I. INTRODUCTION

Graded-refractive-index (GRIN) coatings are coatings that consist of multiple dielectric layers having refractive indices (n) that gradually decrease from the substrate to the ambient.[1] GRIN coatings have been widely used as antireflection (AR) coatings in optical devices such as solar cells[2,3] and light-emitting diodes (LEDs).[4,5] Recently, it has been demonstrated that patterned GRIN coatings can improve the light-extraction efficiency of LEDs by eliminating total internal reflection.[6,7] Such GRIN coatings consist of five layers of varying composition of the transparent dielectrics TiO_2 ($n = 2.5$) and SiO_2 ($n = 1.5$). The GRIN coatings are then patterned into GRIN micropillars with vertical sidewalls through inductively coupled plasma (ICP) reactive ion etching (RIE) using an ITO hard mask.[8]

Furthermore, it was proposed that when compared to GRIN micropillars with *vertical* sidewalls, GRIN micropillars with *tapered* sidewalls can further promote light extraction in LEDs.[9] As shown in Fig. 1, compared to micropillars with *vertical* sidewalls, micropillars with *tapered* sidewalls allow more oblique light rays to strike the sidewalls at near-normal incidence and escape from the LED semiconductor. Thus, more oblique light rays can be directly out-coupled through *tapered* sidewalls than through vertical sidewalls. A more detailed explanation can be found in the earlier literature.[9] A most popular fabrication method for structures with tapered sidewalls is pattern-transfer using thermally reflowed photoresist and dry etching.[10,11] However, it is difficult to fabricate multilayer structures with a large thickness using this method. This is because, during dry etching, the dry-etch-resistance of photoresist is undesirably low. The dry-etch-resistance of photoresist is inversely proportional to the etch rate of photoresist, which in the present study ranges between about 0.1 and 1.0 μm/min. Increasing the thickness of photoresist is not an option since there is a trade-off between the thickness of photoresist and the minimum feature size so that small features would no longer be feasible.

It was reported that photoresist becomes more resistant (mechanically, thermally, and chemically) after ion-implantation (with boron and phosphorus) due to a change of the ion-implanted photoresist to a graphite-like structure.[12,13] In the present paper, we study the effects of Si, N, and Ar ion implantation on the dry-etch-resistance of photoresist. The trend of the measured depth of modification of the photoresist agrees well with the depth simulated by ion-implantation-simulation software (SRIM).[14] Based on the improvement in the dry-etch-resistance of photoresist, we fabricate five-layer GRIN micropillars with tapered sidewalls using the ion-implanted photoresist as an etch mask.

II. EXPERIMENT

In this study, we first process a three-layer GRIN coating into micropillars with tapered sidewalls and then use the results to process an optimized five-layer GRIN coating into micropillars with tapered sidewalls. A three-layer GRIN coating made of TiO_2 and SiO_2 with varying composition in each layer is deposited by co-sputtering on Si substrates.

[a]Electronic mail: mingmafudan@gmail.com
[b]Electronic mail: cho.jaehee@gmail.com

 © 2014 American Vacuum Society

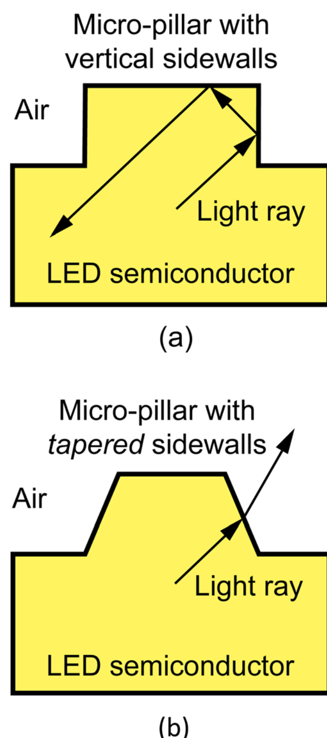

FIG. 1. (Color online) Schematic diagrams of light extraction from a rectangular-parallelepiped-shaped LED with a micropillar with (a) vertical sidewalls and (b) tapered sidewalls.

During the sputter deposition, the Ar and O_2 flow rates are 10 and 0.5 sccm, respectively. The sputter-chamber pressure is kept at 2 mTorr during deposition. The substrate is kept at room temperature. The electrical powers applied to the two sputtering targets are carefully adjusted so that each layer has the desired material composition and refractive index. The thickness and refractive index of each layer is measured by VASE (Variable Angle Spectroscopic Ellipsometry). The measured thickness, measured refractive index, and the material composition (as inferred from VASE) of each layer are shown in Table I for the three-layer and five-layer GRIN coating. As shown in Table I, the thickness of each layer is around 300 nm; thus, the total thickness of the three-layer GRIN coating is around 900 nm and that of the five-layer GRIN coating is around 1.5 μm.

Three-layer GRIN coatings are patterned by contact photolithography using Shipley Company's S1813 photoresist. The patterned photoresist is then reflowed by hard-baking the pattern at 145 °C for 5 min. Each element of the thermally reflowed photoresist pattern has a dome shape. The dome is approximately a hemisphere with a base diameter of 4 μm and a thickness of 1.8 μm. Here, the thickness of the dome-shaped photoresist is defined as the distance between the top of the dome-shaped photoresist and the bottom plane of the photoresist.

In order to study the effects of ion-implantation on the dry-etch-resistance of photoresist, three widely used ion species, Si, N, and Ar ions, are implanted into the S1813

TABLE I. Measured thickness, measured refractive index, and material composition of each layer of the three-layer and the five-layer GRIN coating.

Three-layer GRIN coating	Five-layer GRIN coating	Measured thickness (nm)	Measured refractive index	Material composition
1	1	340	2.6	TiO_2
	2	307	2.2	$(TiO_2)_{0.8}(SiO_2)_{0.2}$
2	3	333	2.0	$(TiO_2)_{0.6}(SiO_2)_{0.4}$
	4	310	1.8	$(TiO_2)_{0.3}(SiO_2)_{0.7}$
3	5	337	1.5	SiO_2

TABLE II. Ion-implantation conditions for the ion-implanted photoresists.

Ion species	1st energy (keV)	Dose (cm^{-2})	2nd energy (keV)	Dose (cm^{-2})	3rd energy (keV)	Dose (cm^{-2})
Si	350	5×10^{15}	225	5×10^{15}	100	5×10^{15}
N	350	5×10^{15}	225	5×10^{15}	100	5×10^{15}
Ar	350	5×10^{15}	225	5×10^{15}	100	5×10^{15}

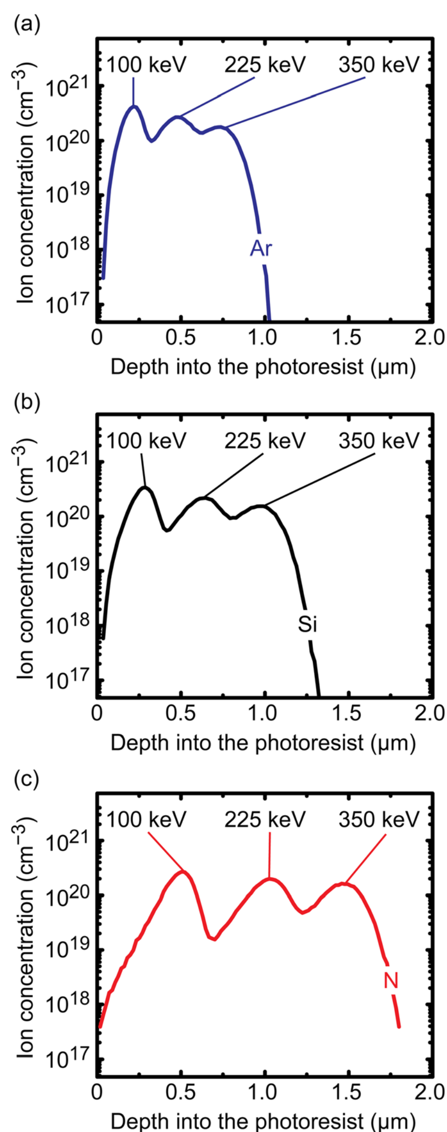

FIG. 2. (Color online) SRIM simulated ion concentration in the photoresist as a function of the depth (into the S1813 photoresist) for (a) Ar, (b) Si, and (c) N implantation at a dose of 5×10^{15} cm^{-2}.

photoresist pattern. The ion-implantation conditions for the ion-implanted photoresists are summarized in Table II. As shown in Table II, the ion-implantation conditions are the same for three ion species: each ion element is implanted using three consecutive implantation steps with each step using the same dose but gradually decreasing implantation energies. The three implantation energies are selected to achieve a more uniform implantation profile throughout the photoresist. For comparison, a reference sample coated with the unimplanted photoresist is also patterned by dry-etching.

The three-layer GRIN coatings are subsequently etched for 150 s under 600 W ICP power, 250 W RIE power, 60 sccm CHF_3, and 15 sccm O_2 with the etch-chamber pressure at 25 mTorr. The fluorine chemistry is selected to achieve smooth sidewalls with a minimum of etch residue.[8] After dry etching, the remaining photoresist and etch residue is removed by immersing the samples into AZ 300t (a photoresist stripper) at 80 °C for 60 min.

III. RESULTS AND DISCUSSION

Figure 2 shows the simulated ion concentration in the photoresist as a function of the depth (into the photoresist) for Ar, Si, and N implantation. The simulation is performed using the SRIM simulator.[14] As shown in Fig. 2, for each type of ion, there are three ion concentration peaks, each of which corresponds to a specific implantation energy. For an implantation dose of $5 \times 10^{15}\,\mathrm{cm}^{-2}$, the peak ion concentrations are within the range of 1×10^{20} to $1 \times 10^{21}\,\mathrm{cm}^{-3}$ depending on energy. In addition, N ions have the largest projected range in the photoresist, while Ar ions have the smallest projected range in the photoresist. This is because for a given energy, the lighter atoms strike the photoresist with a higher velocity and penetrate more deeply into the photoresist.[15] In our experiment, N atoms have the lightest atomic mass among the three elements and thus have the largest projected range in the photoresist; Ar atoms have the heaviest atomic mass among the three elements and thus have the smallest projected range in the photoresist.

Figure 3 shows the cross-sectional scanning electron microscopy (SEM) images of patterned photoresist on the three-layer GRIN coating, which is unimplanted, Si-implanted, N-implanted, and Ar-implanted. Inspection of Fig. 3 shows cross-sections of reflowed photoresist with a homogeneous appearance for the unimplanted photoresist [Fig. 3(a)] but a nonhomogeneous appearance for the implanted photoresists [Figs. 3(b)–3(d)]. That is, there are two distinct regions in the cross-sectional-view of the ion-implanted photoresist dome: an outer shell and an inner core [Figs. 3(b)–3(d)]. This is a clear indication that the structure or composition of the photoresist is affected by the ion-implantation. As shown in Figs. 3(b)–3(d), the outer shell represents the portion of the photoresist that is affected by the ion-implantation, while the inner core represents the portion of the photoresist that is unaffected. Thus, the thickness of the outer shell [i.e., $t_{\mathrm{outer\ shell}}$ as shown in Figs. 3(b)–3(d)] should be proportional to the projected range of ions in the photoresist. Indeed, we can see that the measured

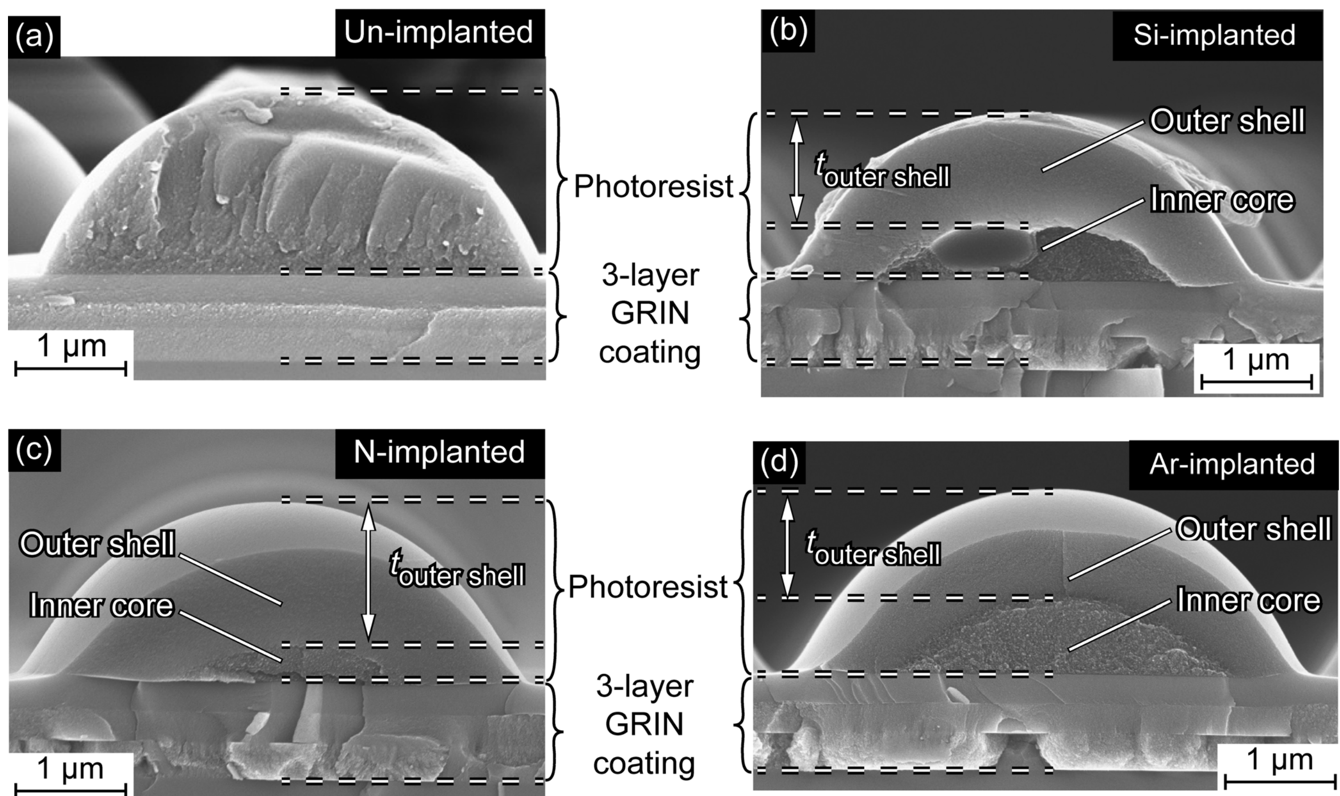

FIG. 3. Cross-sectional scanning electron micrographs of reflowed photoresist domes that are (a) unimplanted, (b) Si-implanted, (c) N-implanted, and (d) Ar-implanted. The domes are located on a three-layer GRIN coating.

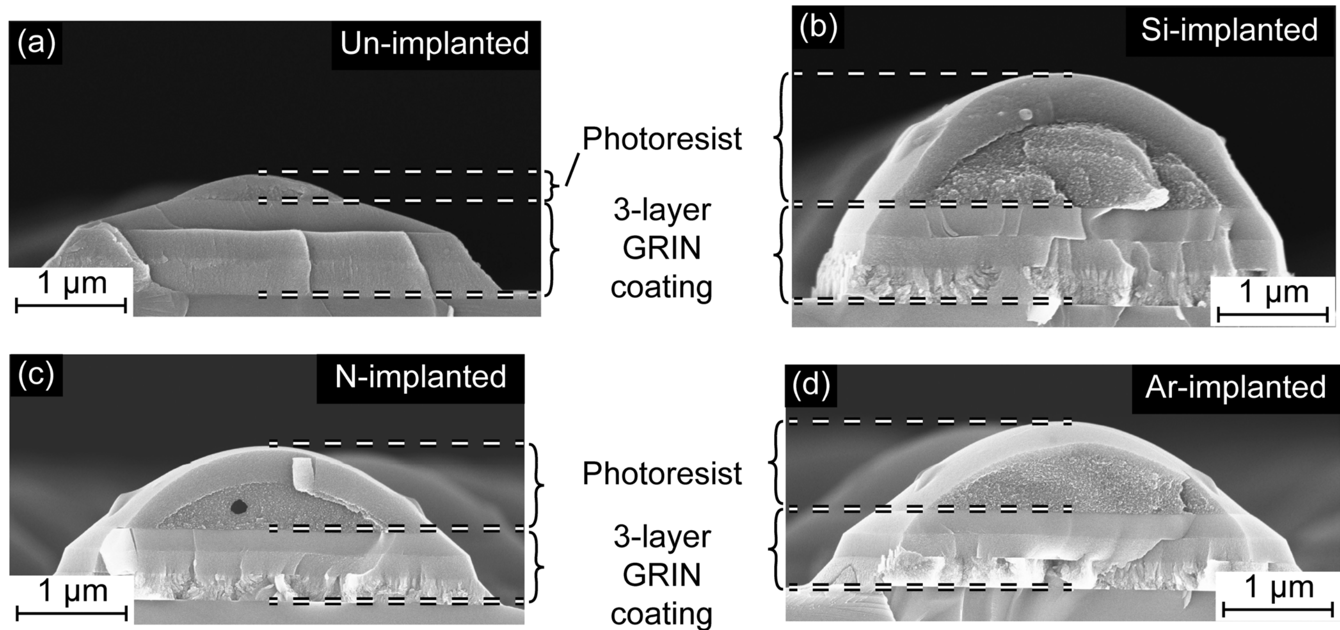

FIG. 4. Post-dry-etching cross-sectional scanning electron micrographs of reflowed photoresist domes that are (a) unimplanted, (b) Si-implanted, (c) N-implanted, and (d) Ar-implanted. The photoresist domes are fabricated on a three-layer GRIN coating that is etched into micropillars.

implantation depth is in good agreement with the trend predicted by the SRIM simulation shown in Fig. 2, i.e., the thickness of the outer shell ($t_{outer\ shell}$) is largest for the N-implanted photoresist and smallest for the Ar-implanted photoresist. The quantitative differences between the simulated thickness (i.e., projected range) and the measured thickness may come from the compositional difference in the photoresist used in the simulation (AZ-111, $C_5H_8O_2$) and in the experiment (the parameters of the proprietary S1813 photoresist are not available in the simulation materials data base).

After dry etching, the GRIN coating is patterned into arrays of GRIN micropillars. Figure 4 shows post-dry-etching cross-sectional SEM images of reflowed domes that are (a) unimplanted, (b) Si-implanted, (c) N-implanted, and (d) Ar-implanted. The domes are located on a three-layer GRIN micropillar. As shown in Fig. 4, the remaining photoresist in the unimplanted sample is minimal (very small thickness), while there is still plenty of remaining photoresist in the ion-implanted samples, indicating the much improved post-implantation dry-etch-resistance of photoresist. Inspection of Fig. 4 also shows that the etch rate of the dielectric GRIN layers is not affected by the ion-implantation.

Next, we quantify the enhancement in the dry-etch-resistance of photoresist. We note that the dry-etch-resistance of photoresist is inversely proportional to the etch rate of photoresist. Thus, a lower etch rate of photoresist indicates a higher dry-etch-resistance of photoresist. Table III summarizes the etch rates of the unimplanted and ion-implanted photoresists. It reveals that the dry-etch-resistance of photoresist is much improved after ion-implantation for all three ion species. The largest enhancement is found for the Si-implanted photoresist, whose etch rate decreases from 0.60 to 0.17 μm/min, i.e., by 72% from that of the unimplanted photoresist.

We notice that although the N ions have the largest projected range in the photoresist, the Si ions result in the largest improvement in the dry-etch-resistance. This, however, cannot be fully explained by the earlier model,[13] i.e., cannot be fully explained by the ion-implanted photoresist changing into a graphite-like structure, since in that case the enhancement in the dry-etch-resistance of photoresist should be directly proportional to the projected range of ions in the photoresist. Our results suggest that, in addition to the reported change of the ion-implanted photoresist to a graphite-like structure, the enhancement of the dry-etch-resistance of photoresist also comes from the newly formed bonds between the photoresist's remaining C atoms and the implanted atoms (i.e., Si, N, and Ar atoms). In our experiments, the Si-implanted photoresist has a larger improvement in dry-etch-resistance than the N- and Ar-implanted photoresist; this is presumably because (i) Si atoms and C atoms have a similar electronic structure; (ii) the implanted Si atoms form stronger chemical bonds with the photoresist's remaining C atoms (higher bonding energy) than the bonds between implanted N and Ar atoms and the photoresist's remaining C atoms;[16] (iii) during implantation, the photoresist presumably cross-linked and incorporated Si atoms into its structure.

Based on the results shown above, we propose the following method to fabricate five-layer GRIN micropillars with *tapered* sidewalls. The method is to use the ion-implanted photoresist that has much improved dry-etch-resistance when used as an etch mask. As a demonstration of the

TABLE III. Measured etch rates of the unimplanted and implanted photoresists.

Ion species	N/A	Si	N	Ar
Etch rate of photoresist (μm/min)	0.60	0.17	0.22	0.23

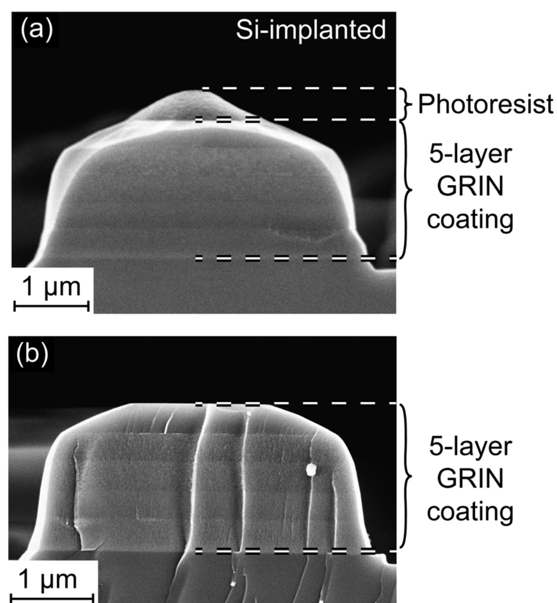

Fig. 5. (a) Post-dry-etching cross-sectional scanning electron micrograph of residual Si-implanted photoresist on top of a five-layer GRIN micropillar. (b) Cross-sectional scanning electron micrograph of a five-layer GRIN micropillar with tapered sidewalls.

method, Fig. 5 shows the cross-sectional SEM images of a five-layer GRIN micropillar with tapered sidewalls fabricated by using Si-implanted photoresist as an etch mask during dry etching. The structure of the five-layer GRIN coating is shown in Table I. The etch conditions are the same as previously mentioned, except for the etch time which is increased to 250 s. As shown in Fig. 5(a), there is still some photoresist remaining after dry etch, once again indicating the much improved dry-etch-resistance for the Si-implanted photoresist. The cross-section of a five-layer GRIN micropillar with tapered sidewalls is shown in Fig. 5(b). Inspection of Fig. 5(b) shows that the taper (i.e., angle of inclination) of the top layer (SiO_2) is larger than that of the lower-lying layers. This is mainly because, during dry etching, the etch mask of the top layer is the photoresist, while the etch mask of a lower-lying layer is the dielectric layer above itself. Even after ion implantation, the dry-etch-resistance of the photoresist is still lower than that of the dielectric layers. Thus, the taper is largest in the top layer. A possible solution is to modify the etch recipe for each layer so that a uniform taper in each layer can be achieved.

IV. SUMMARY AND CONCLUSIONS

In summary, thermally reflowed photoresist, which results in dome-shaped features, is used as an etch mask in ICP RIE of dielectric GRIN coatings. The coatings have varying compositions of TiO_2 and SiO_2 and are used to fabricate GRIN micropillars with tapered sidewalls. The effects of ion implantation on the dry-etch-resistance of photoresist are investigated for Si, N, and Ar ion implantation. Compared with the unimplanted photoresist, the implanted photoresists show enhanced dry-etch-resistance under fluorine chemistry (CHF_3 and O_2). The etch rate of the Si-implanted photoresist is 72% lower than that of the unimplanted photoresist. The measured depth of modification of the photoresist is in good agreement with the trend predicted by SRIM. Our results suggest that in addition to the change of the ion-implanted photoresist to a graphite-like structure, the enhancement of the dry-etch-resistance of photoresist also comes from the newly formed bonds between the photoresist's remaining C atoms and the implanted atoms (i.e., Si, N, and Ar atoms). Using Si-implanted photoresist as an etch mask during dry etching, we demonstrate the fabrication of 1.5-μm-thick five-layer GRIN micropillars with tapered sidewalls.

ACKNOWLEDGMENTS

The authors gratefully acknowledge support by Applied Materials, Samsung Electronics, and the National Research Foundation of Korea Grant funded by the Korean Government (MEST) (NRF-2011-220-D00064). Author J. Cho acknowledges support by the Basic Research Laboratory Program (2011-0027956) and Priority Research Centers Program (2009-0094031) through the National Research Foundation of Korea funded by the Ministry of Education, Science and Technology.

[1]A. Mahdjoub and L. Zighed, Thin Solid Films **478**, 299 (2005).
[2]X. Yan, D. J. Poxson, J. Cho, R. E. Welser, A. K. Sood, J. K. Kim, and E. F. Schubert, Adv. Funct. Mater. **23**, 583 (2013).
[3]S. Chhajed, M. F. Schubert, J. K. Kim, and E. F. Schubert, Appl. Phys. Lett. **93**, 251108 (2008).
[4]J. K. Kim, S. Chhajed, M. F. Schubert, E. F. Schubert, A. J. Fischer, M. H. Crawford, J. Cho, H. Kim, and C. Sone, Adv. Mater. **20**, 801 (2008).
[5]J. K. Kim, A. N. Noemaun, F. W. Mont, D. Meyaard, E. F. Schubert, D. J. Poxson, H. Kim, C. Sone, and Y. Park, Appl. Phys. Lett. **93**, 221111 (2008).
[6]M. Ma, A. Noeumaun, J. Cho, E. F. Schubert, G. B. Kim, and C. Sone, Opt. Express **20**, 16677 (2012).
[7]A. N. Noemaun, F. W. Mont, G. B. Lin, J. Cho, E. F. Schubert, G. B. Kim, C. Sone, and J. K. Kim, J. Appl. Phys. **110**, 054510 (2011).
[8]A. N. Noemaun, F. W. Mont, J. Cho, E. F. Schubert, G. B. Kim, and C. Sone, J. Vac. Sci. Technol. A **29**, 051302 (2011).
[9]M. Ma, J. Cho, E. F. Schubert, Y. Park, G. B. Kim, and C. Sone, Appl. Phys. Lett. **101**, 141105 (2012).
[10]Y. M. Song, S. Y. Bae, J. S. Yu, and Y. T. Lee, Opt. Lett. **34**, 1702 (2009).
[11]S.-H. Park, H. Jeon, Y.-J. Sung, and G.-Y. Yeom, Appl. Opt. **40**, 3698 (2001).
[12]N. Nagai, T. Imai, K. Terada, H. Seki, H. Okumura, H. Fujino, T. Yamamoto, I. Nishiyama, and A. Hatta, Surf. Interface Anal. **33**, 545 (2002).
[13]Y. Okuyama, T. Hashimoto, and T. Koguchi, J. Electrochem. Soc. **125**, 1293 (1978).
[14]J. F. Ziegler, M. D. Ziegler, and J. P. Biersack, Nucl. Instrum. Methods Phys. Res., Sect. B **268**, 1818 (2010).
[15]R. C. Jaeger, *Introduction to Microelectronic Fabrication*, 2nd ed. (Prentice Hall, NJ, 2002).
[16]S. S. Zumdahl and S. A. Zumdahl, *Chemistry*, 5th ed. (Houghton Mifflin College Division, Boston, MA, 1999).